Proceedings of the
8th Graz Brain-Computer Interface Conference 2019 DOI: 10.3217/978-3-85125-682-6-22

EEG SOURCE ANALYSIS OF VISUAL MOTION IMAGERY FOR APPLICATION TO BRAIN-COMPUTER INTERFACE

K. Koizumi[1], K. Ueda[1], N. Tateyama[1], M. Nakao[1]

[1] Department of Mechanical Engineering, Graduate School of Engineering, The University of Tokyo, Tokyo, Japan

E-mail: koizumi@hnl.t.u-tokyo.ac.jp

ABSTRACT: In the field of brain-computer interface (BCI) research, building more intuitive and goal-directed BCI systems is a key to breakthrough. "Visual motion imagery," which enables visual imaging of the operation of a target is one possible method for application to BCI. As a foothold study for applying visual motion imagery to BCI, we examined EEG source activity during visual motion imagery via comparison with visual motion perception. Source activities induced in beta band activity in the right posterior cingulate, left precuneus and left cuneus, and in low gamma activity in the right inferior parietal lobule and supramarginal gyrus were significantly higher in visual motion imagery than in visual motion perception. These findings identify promising brain areas for feature extraction for the development of BCI using visual motion imagery.

INTRODUCTION

Brain-computer interface (BCI) technology enables direct communication between the brain and a computer. When the aim is to control devices such as a computer cursor and wheelchair with electroencephalography (EEG)-based BCI, most studies have used P300 evoked potential, several steady-state visual evoked potentials (SSVEPs), and sensory-motor imagery. These conventional approaches are well established, but technological problems remain. To obtain a P300 or SSVEP signal, users must constantly concentrate on watching an external stimulus presented on a monitor. On the other hand, sensory-motor imagery requires a long training time and, because brain signals related to the user's body movement are used to operate devices, multiclass control is difficult. In the BCI development, it is also important to search for new approaches that are more goal-directed and intuitive for users compared to conventional methods.

Visual motion imagery, which involves visualization of a target operation is one approach used in recent studies [1,2]. Understanding brain source activity is a key for practical application of any new BCI approach, and this understanding contributes not only to the field of BCI but also to the field of neuroscience. However, few studies investigated brain activity and mechanism during visual motion imagery using EEG.

In this study, we examined source localization during visual motion imagery using exact low-resolution brain electromagnetic tomography (eLORETA) and compared findings with visual motion perception**.** Our aim was to clarify differences in brain activity between imagery and perception. Details regarding the experiment are provided in the MATERIALS AND METHODS section; Statistical analysis results of the differences in source activities between imagery and perception are detailed in the RESULTS section.

MATERIALS AND METHODS

Participants: A total of 18 healthy male subjects participated in the experiments. Two participants were removed from the final analysis: one due to a technical error during recording, and one due to excessive noise in the EEG data. Fifteen of the 16 remaining participants were right-handed; one was left-handed. The average age of participants was 22.9 years (standard deviation, 2.2, range, 20-29 years). All participants had normal or corrected-to-normal vision. The experimental procedure was approved by the Research Ethics Committee of the Graduate School of Engineering, the University of Tokyo, Tokyo, Japan (approval number; KE17-31). All participants provided written informed consent prior to their participation in this study.

Experimental equipment: EEG recordings were performed in a shielded room, where participants were seated in a comfortable chair approximately 90 cm from a 76.2 cm screen (MultiSync LCD-PA302W, NEC Corp) with an effective display area of 641 × 401 mm. Participants were instructed to relax and refrain from excessive body or head movements. They were also instructed to fix their gaze on the middle of the monitor.

Experimental Procedure: During imagery, participants visually imagined the movement of a drone in three planes (up/down, left/right, and forward/backward) while watching a drone hovering at the center position of three-dimensional space presented on the monitor. To reduce individual differences in imagination and perception, immediately before each imagination, participants watched a movie in which the same drone moved in one direction (Fig. 1). The three-dimensional space was displayed at a 32° visual angle in width and 20° in height at the center of the monitor. Initially, the drone subtended 6.0° in width by 2.5° in height, hovering at the center position. It then moved in

 DOI: 10.3217/978-3-85125-682-6-22

one direction for 4 s (up/down at 0.83°/s, left/right at 1.53°/s, forward/backward at 0.51°/s). When the drone moved forward or backward, its size was gradually reduced to 60% or increased to 140% at a constant speed. The movie was presented for 4 s (perception time), the fixation point was presented for 1 s, then the hovering-drone image was presented for 4 s (imagery time) (Fig.2). Participants were instructed to reproduce the same movement they had observed during the perception time in the imagery time of each trial. Six trials defined one set, and the order of the six directions in each set was random. The entire task consisted of ten sets.

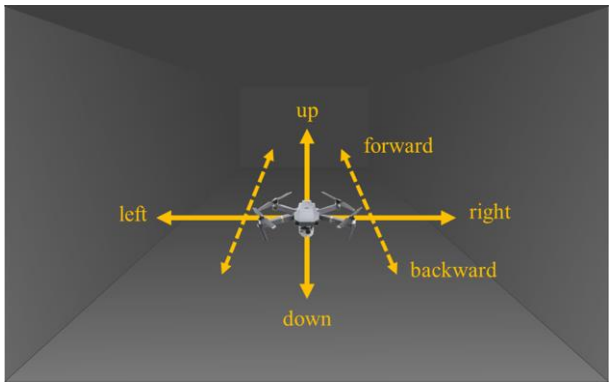

Figure 1: Illustration of the movie shown to participants

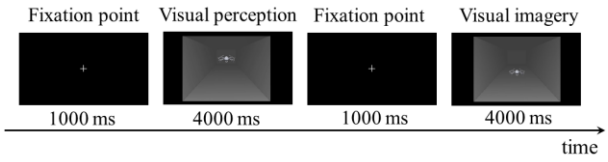

Figure 2: Experimental paradigm

Data acquisition: EEG signals were continuously recorded at a sampling rate of 1 kHz using an EEG system (EEG-1200, Nihon Kohden Corp., Tokyo, Japan). Electrodes were located at 65 positions according to the extended 10-20 system (Fig. 3). Two additional electrodes were fixed on the participant's earlobes (A1, A2) as references.

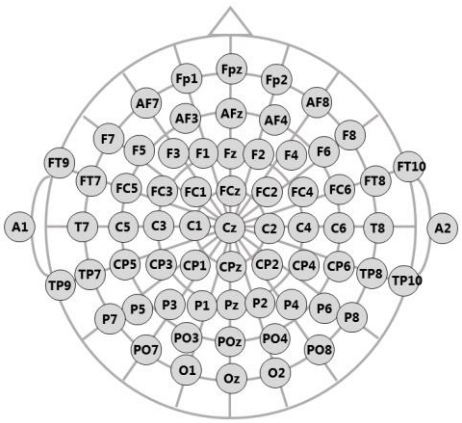

Figure 3: The 65 electrode locations of the extended 10-20 system and two electrodes (A1, A2) on the earlobes

Signal preprocessing: Data were analyzed offline using MATLAB® 2016b and EEGLAB (Delorme & Makeig, 2004) version 14.1.b. Recorded EEG signals were filtered between 1 Hz and 120 Hz using a 3300th-order finite impulse response filter, and powerline fluctuations at 50 Hz were removed using the Cleanline EEGLAB plug-in Electrooculographic artifacts due to blinks or eye movements and electromyographic (EMG) artifacts were removed using the Automatic Subspace Reconstruction (ASR) method implemented in the 'clean_rawdata' plugin of EEGLAB [3]. The threshold of ASR was set at 15 standard deviations with all the other parameters turned off. Single-trial epochs were extracted from −500 to 4000 ms relative to stimulus onset. Baseline was set as the mean signal 500 ms before onset of an perception or imagery period.

EEG source localization: The eLORETA was used to compute the intracortical distribution of current source density from multichannel head-surface EEG data [4]. Validation of LORETA for localization agreement with multimodal imaging techniques is reported in several published studies [5-7]. Further, previous research reported that eLORETA performs well in terms of less localization error and visibility compared to other low-resolution techniques (sLORETA) [8]. The head model and electrode coordinates were based on the Montreal Neurologic Institute average MRI brain (MRI152). Solution space was restricted to the cortical gray matter (6239 voxels at 5×5×5 mm spatial resolution). eLORETA functional images were computed for each subject in each of the following 6 frequency bands: delta (0.5-3.5Hz); theta (4-7.5Hz); alpha (8-12.5Hz); beta (13-30Hz); low gamma (30.5-60Hz); high gamma (60.5-120Hz). Considering differences in brain activity among participants, subject-wise normalization was performed before statistical analysis. This normalization used total power over all frequency bands and over all voxels from a participant to unity.

Statistical analysis: We used movement in six directions to investigate imagined direction classification for future BCI applications. However, our aim was to clarify differences in brain activity between imagery and perception. Hence, we did not distinguish state by direction. Thus, for source localization, we used imagery time as the period that participants visualized movement of the drone regardless of the imagined movement direction. Similarly, we used perception time as the period that participants watched the movement of the drone regardless of the movement direction. The differences of cortical source localization between conditions were assessed in each frequency band with voxel-by-voxel paired *t*-tests of log-transformed power. Randomized statistical nonparametric mapping (SnPM) was applied to determine critical probability threshold values for observed *t*-values with correction for multiple comparisons over all voxels and all frequencies [9]. A total number of 5000 permutations were used to determine the significance for each randomization test.

 DOI: 10.3217/978-3-85125-682-6-22

RESULTS

Fig. 4 shows differences in brain activity in each frequency band between imagery and perception. The color becomes redder as brain activity during imagery is higher than during perception. The color becomes bluer as the brain activity during perception is higher than during imagery. In the delta and theta band, activity in the frontal lobe was relatively higher during perception, and activity over a large area of the parietal and occipital lobes was relatively higher during imagery (Fig. 4 (a), (b)). In the alpha band, activity in the left frontal lobe and parietal lobe, mainly on postcentral gyrus and inferior parietal lobule (Broadmann area 2, 3, 40), was relatively higher during visual perception, and activity in the left occipital lobes, mainly the cuneus and precuneus (Broadmann area 18, 23, 31), was relatively higher during imagery (Fig. 4 (c)). In the beta band, the activity in the right limbic lobe and left occipital lobe, mainly on the right posterior cingulate, the left cuneus and the left precuneus (Broadmann area 23, 7, 31), were relatively higher during imagery (Fig. 4 (d)). In the low gamma band, activity in the right parietal lobe and right temporal lobe, mainly in the inferior parietal lobule, superior temporal gyrus and supramarginal gyrus (Broadmann area 40, 39,) were relatively higher during imagery (Fig. 4 (e)). In the high gamma band, activity in the right frontal lobe (Broadmann area 8, 9), was relatively higher during visual perception and activity on the right parietal lobe and right temporal lobe, mainly on the inferior parietal lobule, the superior temporal gyrus, the precuneus and the angular gyrus (Broadmann area 40, 39, 7). were relatively higher during imagery (Fig. 4 (f)).
Two-tailed *t*-tests showed significant differences between imagery and perception conditions in the beta and low gamma band ($p < 0.05$ for *t*-values above 5.22, corrected for multiple comparisons). Current density in the beta band for imagery was significantly higher in the right posterior cingulate (Broadmann area 23, 30), in the left precuneus (Broadmann area 7, 31) and in the left cuneus (Broadmann area 7) compared to perception (Fig. 5(a), Tab. 1). In the low gamma band, activities in the right inferior parietal lobule and right supramarginal gyrus (Broadmann area 40), were significantly higher for imagery compared perception (Fig. 5(b), Tab. 1).

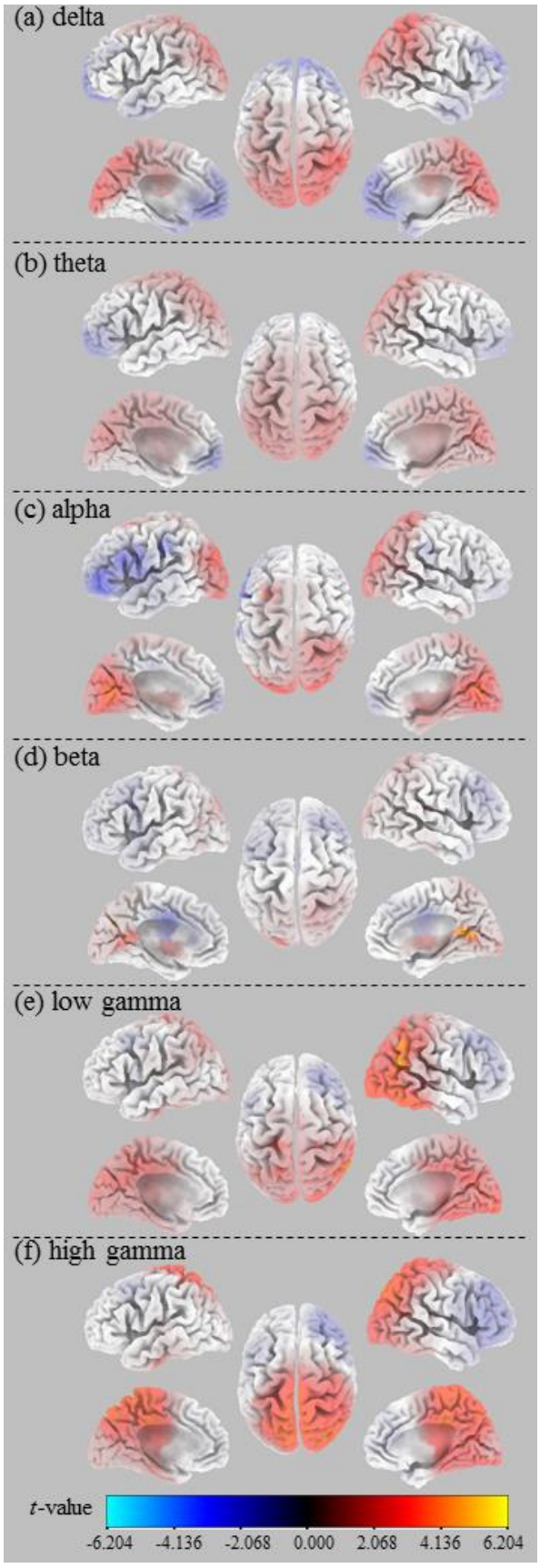

Figure 4: The difference of brain activity between imagery and perception in each frequency band ((a) delta, (b)theta, (c) alpha, (d) beta, (e) low gamma, (f) high gamma).

 DOI: 10.3217/978-3-85125-682-6-22

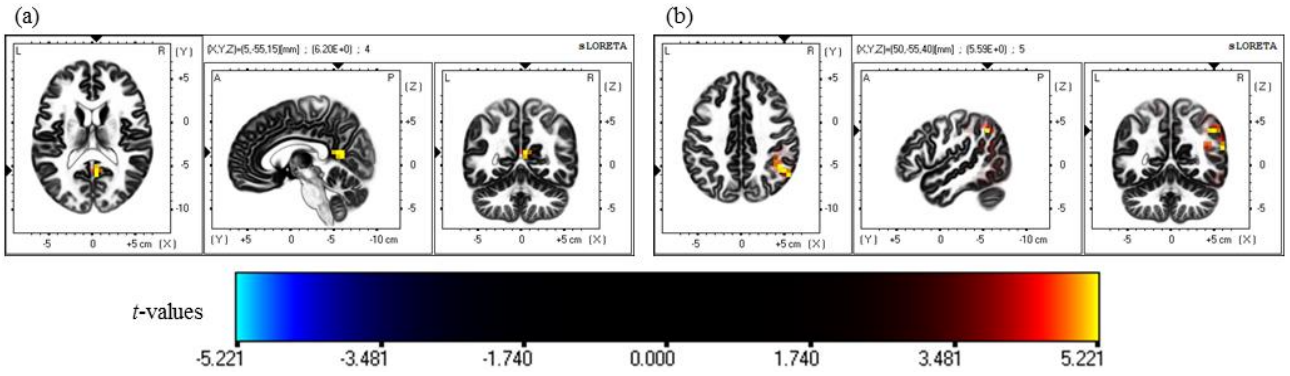

Figure 5: Significant differences in source current density between imagery and visual perception (red-coded and deep blue-coded for $p < 0.10$, $|t| > 4.75$; yellow-coded and light blue-coded for $p<0.05$, $|t| > 5.22$, corrected for multiple comparison). (a) Differences in the beta frequency band. (b) Differences in the low gamma frequency band. The color becomes yellower as brain activity in imagery is significantly higher than perception, and the color becomes bluer as the brain activity in perception is significantly higher than in imagery.

Table 1: Brain areas activated during imagery that are significantly higher than during perception

Brain Area	Broadmann area	MNI coordinate (mm)			Frequency band	*t*-value
		X	Y	Z		
Limbic Lobe, Posterior Cingulate	23	5	-55	15	Beta	6.20
	30	5	-60	10	Beta	5.49
	23	5	-60	15	Beta	5.29
Parietal Lobe, Precuneus	31	-15	-70	25	Beta	6.00
	7	-15	-70	30	Beta	5.74
Occipital Lobe, Precuneus	31	-15	-65	25	Beta	5.82
Occipital Lobe, Cuneus	7	-15	-75	30	Beta	5.68
Limbic Lobe, Precuneus	31	-15	-60	25	Beta	5.56
Parietal Lobe, Inferior Parietal Lobule	40	50	-55	40	Low gamma	5.59
	40	55	-60	40	Low gamma	5.25
	40	45	-50	40	Low gamma	5.22
Temporal Lobe, Supramarginal Gyrus	40	60	-55	20	Low gamma	5.30

t-value is the value of the statistical comparison with $p < 0.05$ for *t*-value above 5.22.

DISCUSSION

In the present study, we used eLORETA to identify brain regions where activation is associated with imagery via comparison to perception. Source activities induced in the beta band in the right posterior cingulate, left precuneus and left cuneus, and low gamma activity induced in the right inferior parietal lobule, and right supramarginal gyrus was significantly higher for imagery than perception.

There was no significant difference between perception and imagery in the alpha band where the signal-to-noise ratio is rather high. We speculate that the visual attention to the imagined movement of the drone induced the decrease in the alpha band activity in the same degree as the perceptual movement.

The precuneus is activated in several visual imagery studies using PET or functional MRI [10,11]. In this study, we used EEG for data acquisition and were able to observe the activity of precuneus induced by visual imagery. The precuneus (Broadman area 7,31) is known to have intimate interconnection with the posterior cingulate (Broadman area 23,31) and selective connections with the inferior parietal lobule and intraparietal sulcus. The latter is known to be important in visuospatial information processing [12]. Further, the ventro-dorsal stream, a processing pathway for visual information that reaches the primary visual cortex, proceeds to the inferior parietal lobule and is related to position and movement analysis of an object and to conscious of the object [13]. During perception, a participant is only watching movement of the drone, but during imagery, it is necessary to recall movement of the drone and produce a virtual visual image in the brain. We speculate that this difference in visuospatial information processing load strengthens the brain connection we describe above, and consequently, some brain areas, such as the posterior cingulate and inferior parietal lobule display significantly increased activity during imagery. Previous studies have reported that posterior cingulate is related to memory recall [14,15]. We used EEG and were able to observe the activity of posterior cingulate by visual imagery. From this result, we speculate that the participants were recalling the movie they watched

 DOI: 10.3217/978-3-85125-682-6-22

immediately before the imagery period.

CONCLUSION

We studied EEG source activity of visual motion imagery via comparison with visual motion perception. We found brain activity particular to visual motion imagery in the posterior cingulate, precuneus, cuneus, inferior parietal lobule, and supramarginal gyrus. Based on these results, we will analyze functional connectivity between brain regions related to visuospatial information processing in the future work. In addition, visual motion imagery may be a useful new approach to BCI. Therefore, we hope to investigate the possibility of classification of imagined directions focusing on the brain areas where increased activity was observed during visual motion imagery.

REFERENCES

[1] Sousa T, Amaral C, Andrade J, Pires G, Nunes UJ, Castelo-Branco M. Pure visual imagery as a potential approach to achieve three classes of control for implementation of BCI in non-motor disorders. J. Neural Eng. 2017;14(4): 046026.

[2] Koizumi K, Ueda K, Nakao M. Development of a Cognitive Brain-Machine Interface Based on a Visual Imagery Method, in Proc. EMBC'18, Honolulu, HI, USA, 2018, 1062-1065

[3] Mullen T, Kothe C, Chi YM, Ojeda A, Kerth T, Makeig S, ... & Jung TP. Real-time modeling and 3D visualization of source dynamics and connectivity using wearable EEG, in Proc. EMBC'13, Osaka, Japan, 2013, 2184-2187

[4] Pascual-Marqui, RD, Lehmann D, Koukkou M, Kochi K, Anderer P, Saletu B, ..., Biscay-Lirio R. Assessing interactions in the brain with exact low-resolution electromagnetic tomography. Philosophical Transactions of the Royal Society A: Mathematical, Physical and Engineering Sciences. 2011;369(1952):3768-3784.

[5] Mulert C, Jäger L, Schmitt R, Bussfeld P, Pogarell O, Möller HJ, Juckel G, Hegerl U. Integration of fMRI and simultaneous EEG: towards a comprehensive understanding of localization and time-course of brain activity in target detection. Neuroimage. 2004;22(1): 83–94

[6] Worrell GA, Lagerlund TD, Sharbrough FW, Brinkmann BH, Busacker NE, Cicora KM, O'Brien TJ. Localization of the epileptic focus by Low-Resolution Electromagnetic Tomography in patients with a lesion demonstrated by MRI. Brain Topography. 2000;12(4): 273–282

[7] Zumsteg D, Wennberg RA, Treyer V, Buck A, Wieser HG. H215O or 13NH3 PET and electromagnetic tomography (LORETA) during partial status epilepticus. Neurology. 2005;65(10): 1657–1660

[8] Jatoi MA, Kamel N, Malik AS, Faye I. EEG based brain source localization comparison of sLORETA and eLORETA. Australas. Phys. Eng. Sci. Med. 2014;37(4): 713-721.

[9] Nichols TE, Holmes AP. Nonparametric permutation tests for functional neuroimaging: a primer with examples. Human Brain Mapping. 2002;15(1): 1-25

[10] Mellet E, Petit L, Mazoyer B, Denis M, Tzourio N. Reopening the mental imagery debate: lessons from functional anatomy. Neuroimage. 1998; 8(2): 129–139.

[11] Ishai A, Haxby JV, Ungerleider LG. Visual imagery of famous faces: effects of memory and attention revealed by fMRI. Neuroimage. 2002; 17(4): 1729–1741.

[12] Cavanna AE, Trimble MR. The precuneus : a review of its functional anatomy and behavioral correlates. Brain. 2006;129(3): 564-583

[13] Gallese V. The "conscious" dorsal stream: embodied simulation and its role in space and action conscious awareness. Psyche. 2007;13(1): 1-20

[14] Maddock RJ, Garrett AS, Buonocore MH. Remembering familiar people: the posterior cingulate cortex and autobiographical memory retrieval. Neuroscience. 2001;104(3): 667-676.

[15] Sutherland RJ, Hoesing JM. Posterior cingulate cortex and spatial memory: A microlimnology analysis. In Neurobiology of cingulate cortex and limbic thalamus. Birkhäuser, Boston, MA 1993, pp. 461-477